IJCPE

Evaluation the Effect of Velocity and Temperature on the Corrosion Rate of Crude Oil Pipeline in the Presence of CO₂/H₂S Dissolved Gases

Haider Hadi Jasim

Chemical engineering department, College of engineering, Basrah University, Basrah, Iraq

Abstract

In this paper investigate the influences of dissolved CO_2/H_2S gases, crude oil velocity and temperature on the rate of corrosion of crude oil transmission pipelines of Maysan oil fields southern Iraq. The Potentiostatic corrosion test technique was conducted into two types of carbon steel pipeline (materials API 5L X60 and API 5L X80). The computer software ECE electronic corrosion engineer was used to predict the influences of CO_2 partial pressure, the composition of crude oil, flow velocity of crude oil and percentage of material elements of carbon steel on the rate of corrosion. As a result, the carbon steel API 5L X80 indicates good and appropriate resistance to corrosion compared to carbon steel API 5L X60. The rate of corrosion acquired from the test in flow conditions is most significant than that in static conditions. The crude oil from Noor field has the largest value of corrosion rate, while the crude oil from Halfaya field has the lower value; other crude oils have moderate values. The dissolved CO_2/H_2S gases contribute by a low degree in internal pipeline corrosion because of the small concentrations.

Keywords: *CO₂/H₂S corrosion, crude oil velocity, chloride salts, Potentiostatic test, carbon steel*

1- Introduction

The pipelines are used to transport a crude oil or its products from one location to every other. Depending on the purpose, the oil pipelines can be labeled into three categories. First, gathering lines, this type has a small diameter and is used in short distances to handle crude oil. Second, transportation pipelines or feeders have a diameter greater than gathering pipelines and pass the oil product from storage or refinery units to distribution pipelines. Thirdly, a transmission pipeline, this type has the largest diameter and used to transport various grades of crude oil from the production area to the ultimate consumption area [1].

Crude oil is a complex mixture contains different impurities which effect on the corrosion rate of metal such as sulfur, water, various dissolved ions (Na^+, K^+, Ca^{+2}, SO_4^{-1}, Cl^- …etc), organic acids, CO_2 and H_2S gases. Corrosion of carbon steel by CO_2 gas is a significant problem in the crude oil transportation pipelines; CO_2 gas dissolves in the water at different extents depending on temperature and pressure, which producing corrosive species. These species, besides the conventional salinity, producing the weak carbonic acid (H_2CO_3), bicarbonate (HCO_3^-) and carbonate (CO_3^{-2}) and becomes as driving the corrosion reactions depending on their concentrations and on pH levels [2], [3].

The electronic corrosion engineer (ECE) software is a good new tool that provides a useful approach for estimating the rate of corrosion of CO_2 and H_2S dissolved gases on different types of carbon steel material used in a pipeline and tubes for crude oil transportation. Various parameters that influence the corrosion in the presence of CO_2 was taken by the ECE program include the CO_2 partial pressure, temperature, and the crude oil velocity [4].

The potentiostatic technique is one of the best electrochemical techniques used in corrosion testing for a quick time. This method includes the application of anodic discrete potential values in the scope of ± 250 mV to the immersed specimen in a solution for a fixed time, and the potential-log current density curve is obtained. Analysis of the curve using Tafel technique can result in the corrosion current, which is used to calculate the value of corrosion rate [5], [6].

The problems of CO_2 corrosion and its control of oil pipelines have been reported in many studies. Vuppu et al. [7] studied the influence of temperature on the rate of corrosion and forms of protective carbonate layer on carbon steel pipelines at various crude oil velocities and oil-water mixtures. They show that both increases the temperatures and oil velocities have negative effect on protective carbonate layer formed on the steel surface. Xu et al. [8] review the corrosion mechanism of CO_2, H_2S and SO_2 of the inner side of oil pipelines.

Corresponding Authors: Name: Haider Hadi Jasim , Email: raidhani73@yahoo.com

Their results show that the corrosion occurs as a result of the reactions between the crude oil compounds and the inner side of the pipelines through crude oil transport. Prakash et al. [9] study the internal corrosion of the API 5L Grade-B carbons steel metal of Kuwait export crude oil pipeline network. Results of their study showed that in addition to the microbial effects, corrosion problems are caused by the effect of CO_2 and H_2S gases. Saleh et al. [10] studied the corrosion rate of carbon steel pipe under various conditions including salinity, temperature velocity for both single and multiple flows of crude oil.

Their result's shows that for a single phase flow, the rate of metal corrosion in the NaCl brine solution is larger than in the multiphase flow (NaCl brine - CO2 - kerosene). Wang et al. [11] reviewed and summarized the methods of measuring thecorrosion in oil-brine mixed conditions.

They show that the effects of water and wetting behavior in corrosion process were very impressive in the case of flow conditions. Muhammed [12] investigated the effects of soil properties contains by crude oil on the corrosion rate of API X70 steel pipeline used in oil transmissions from Iraq to Turkey.

The results showed that the soil's moisture content and pH had the most significant impact on the corrosion process. Mobbassar et al. [13] demonstrated the factor influencing CO_2 corrosion in inner oil pipeline made from low carbon alloy steel. They showed that analyzing the final corrosion product can help to select the most efficient and economical materials resistant to corrosion in the CO_2 environment.

Mursalov [14] review the corrosion mechanism of H_2S, the effect of pH value and temperature on the corrosion rate in the oil industry. The results of studies show that various oxides and chemical compounds are formed on the metal surface depending on the H_2S concentration, pH value, and temperature and CO_2 presence in the oil solutions.

Cedeno et al. [15] study by using the electrochemical measurements the effects of fluid speed, temperature and oil content on the corrosion rate of the AISI-SAE 1020 steel used in the petroleum transportation pipelines under a saturated CO_2 gas.

The results show that crude oil has the most significant effect of in the rate of corrosion of steel and increased as temperature and fluid velocity increased. Kolawole et al. [16] give a comprehensive review of CO_2 and H_2S corrosion problems in API 5L steel pipeline and the proper methods to control the corrosion problems. They showed that the primary causes of corrosion in oil and gas pipelines are the presence of water together with acid gases (CO_2 and H_2S).

This research aims to study the corrosion phenomenon of two types of carbon steel pipeline API 5L X60 and API 5L X80 used for the transport of crude oil through the use of Potentiostatic corrosion test method. Engineering corrosion software version 5.1 was used to calculate the rate of CO_2/H_2S corrosion of crude oil pipelines underneath different water fractions, temperature, velocity, and pressure of crude oil.

2- Experimental Methods

2.1. Pipeline Materials and Specimens Preparation

In Iraq, there are two networks of pipelines extending over a distance of 300 km and transport crude oil from Maysan oil fields (Buzerkan, Halfaya and Faqa oil fields) to the port of Basrah southern Iraq.

The networks pipeline materials are seamless carbon steels API 5L X80 and API 5L X60 and the chemical compositions are given in Table **1** and Table **2**, respectively. The mechanical properties of these two materials are listed in Table **3**.

The API 5L X80 pipelines have a diameter of 122 cm, and the API 5L X60 have a diameter of 61 cm. Both of these pipelines have a thickness of 14 mm.

Table 1. Chemical composition (wt. %) of API 5L X80 carbon steel [17]

Metals	%	Metals	%
C	0.08	Al	0.03
Si	0.26	Mo	0.27
Mn	1.75	Ni	0.22
P	0.011	Nb	0.07
S	0.0005	Fe	Balance

Table 2. Chemical composition (wt. %) of API 5L X60 carbon steel [18]

Metals	%	Metal	%
C	0.007	Al	0.008
Si	0.22	Cu	0.013
Mn	1.63	Ti	0.010
P	0.01	V	0.072
S	0.005	Nb	0.052
Cr	0.011	N	0.008
Ni	0.011	Mo	0.228

Table 3. Mechanical properties of API 5L X80 and API 5L X60 carbon steel [17], [18]

Grade	Yield strength MPa (Min.)	Tensile strength MPa	Elongation % (Min.)
X80	555 Min.	625- 700	20 Min.
X60	541 Min.	627	27 Min.

The test specimens were prepared by cutting it in a cylindrical shape from a plate pipe material with a diameter of 1 cm and a thickness of 5 mm.

According to ASTM G1-03 [19] and ASTM G59-97 [20], the specimens were sequentially polished using silicon abrasive papers of 160, 180 and 200 grades, then washed with distilled water and dried with hot air in ambient conditions.

The specimens are shown in Fig. **1**. For each test, a new specimen was used for testing, a total of 50 specimens were used.

Fig. 1. Specimens for Potentiostatic test: A- X60 Carbon steel B- X80 Carbon steel

2.2. Crude Oil Samples Analysis

The test oil samples used in this study were obtained from different oil fields in Maysan province (Noor, Buzerkan, Halfaya, Abu-Gharab, Faqa1 and Faqa2) southern Iraq. The material compositions of crude oils are analyzed in Nahr Umer laboratory of the south oil company and are listed in Table **4**. The physical properties of crude oils obtained from field's laboratory are summarized in Table **5**.

Table 4. Compositions of various crude oils

Materials	Fields					
	Noor	Bazerkan	Faqa1	Faqa2	Halfaya	Abu-Garab
Iron ppm wt.	1.1	2.2	3.76	3.9	2.8	1.77
Copper ppm wt.	6.1	3	5.1	5.2	3.6	1.3
Vanadium ppm wt.	30	32	31	31	34	29
Nickel ppm wt.	8.7	10	11	11.6	7.1	11
Cadmium ppm	0.78	0.41	0.52	0.64	0.23	0.8
Aluminum ppm wt.	0.44	0.13	0.31	0.33	0.16	0.27
Manganese ppm wt.	0.30	0.17	0.22	0.22	0.27	0.10
Sulfur %	4.6	5.12	3.89	3.9	4.85	4.86
Water content %	2.4	1.85	1.96	2.05	2	2.3
NaCl ppm	44	31.5	24.4	22.3	14	11
H_2S (g) ppm	0.32	0.21	0.42	0.40	0.49	0.45
CO_2 (g) ppm	0.96	0.41	0.67	0.77	0.57	0.83

Table 5. Physical properties of crude oils

Properties	Fields					
	Noor	Bazergan	Faqa1	Faqa2	Halfaya	Abu -Gharab
API	62	24.7	22.5	23.2	27	25
Asphaltenes %	13.8	13.2	10.5	12.6	15.1	14.8
Specific gravity at 20°C	0.8792	0.8901	0.9048	0.9128	0.8835	0.8584
Kinematics viscosity cst at 20°C	33.5	45	40.1	33.6	44	39
Dielectric Constant	2.52	1.78	2.11	2.02	1.92	971.

2.3. Potentiostatic Corrosion Test Techniques

Fig. **2** demonstrates the collection of Potentiostatic corrosion test equipment includes (computerized M-Lap Potentiostatic, water bath and three electrodes corrosion cell. The three corrosion cell electrodes are a working electrode (the sample material), a counter electrode (Platonized Titanium (Pi-Ti)), and the Ag/AgCl reference electrode. Fig. **3** shows the electrochemical flow cell used in Potentiostatic test.
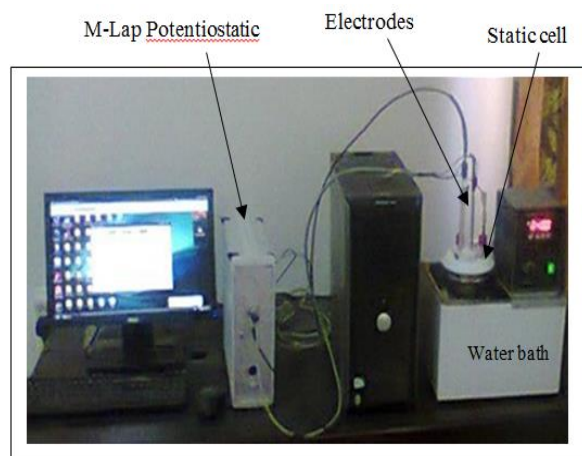
Fig. 2. M-Lap Potentiostatic test collection
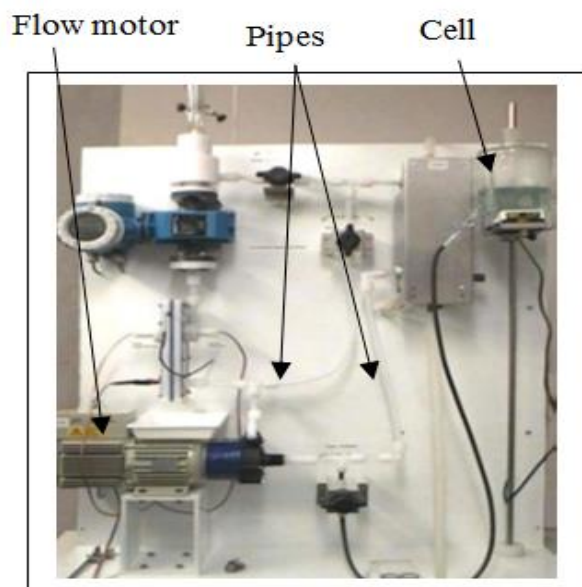
Fig. 3. Electrochemical flow cell

Due to the low conductivity of crude oil, the Potentiostatic corrosion test of the two types of pipelines material in crude oil is impossible. This test can increase the conductivity of crude oil through the use of the Potter method for conducting the Potentiostatic test [21].

In the Potter method, a small quantity of toluene (methylbenzene $C_6H_5CH_3$) was added to the crude oil solution.

The toluene is a solvent and selected for two reasons: first, the boiling point of the toluene must be higher than 60°C and secondly, it must be causing the minimum interference.

According to the Potter method, a 30 ml Toluene was added to 500 ml of crude oil and then added water to crude oil until the total water percentages reached to 5%. Then mix the results with a mixer to make sure the mixture is very well mixed and put it in the glass cell.

A ligament is a round glass cell is used to ensure that the test electrolyte medium is isolated from the air environment. The glass cell is inserted into a temperature controller bath containing water solution and maintained constant (within ± 0.1 °C) to control the test solution temperature.

For conducting Potentiostatic corrosion test, the specimen shall be a run under open circuit conditions for an exposure period of 60 minutes and the potential has been recorded at the end of the exposure period. The potential of ±250 mV is then applied to the measured open circuit potential of the working electrode at a scan rate of 0.5 mV/s. During the corrosion testing, a Potentiostatic test is carried out for a total time of 1 hour and new crude oil and new specimen are used for each test.

The computer-operated and controlled M-Lap Potentiostatic device was used to record data (current, voltage and test time) during the test. The M-Lap science Bank-Electronics program version 5.1.exe is used.

The output of the experiment test is a graph of the log current versus the potential plot. The curves result are analyzed using Tafel linearization method and final output can produce the corrosion current $I_{cor.}$. Using the corrosion current density $i_{cor.}$, the rate of corrosion (C_r) in mm/year was estimated by the following equation [22]:

$$C_r = 3.27 * 10^{-3} * \frac{i_{cor.}}{\rho_m} E_w \qquad (1)$$

And

$$i_{cor.} = \frac{I_{cor.}}{A_s} \qquad (2)$$

Where,

A_s: Surface area of the specimen (cm^2).
ρ_m: Density of metal (g/cm^3).
I_{cor} : Corrosion current obtained from Tafel extrapolation method.

The equivalent weight (E_w) is given by the following relation [23]:

$$E_w = \frac{1}{\sum \frac{n_i F_i}{A_i}} \qquad (3)$$

Where,

A_i : Atomic mass of the tested metal (g/mol).
n_i : Valiancy.
F_i : Mass fraction of alloying elements.

3- Model of CO$_2$ Corrosion Rate Calculation

The corrosion model in the ECE program is based on the de Waard-Lotz corrosion model and two cathodic reactions are recognized [24], [25]:

$$H^+ + \text{electron} \longrightarrow 0.5\,H_2 \qquad (4)$$

$$H_2CO_3 + \text{electron} \longrightarrow 0.5\,H_2 + HCO_3^- \qquad (5)$$
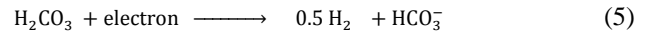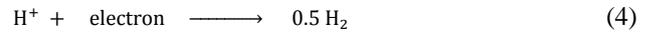
The metal anodic dissolution reaction balances the flow of electrons from these reactions, i.e.

$$Fe \longrightarrow Fe^{+2} + 2\,electrons \qquad (6)$$
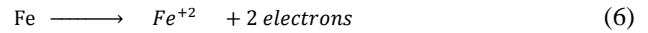
The basic rate of CO2 corrosion (Vcor.) is the combination of these two processes and given as:

$$V_{cor.} = \frac{1}{\frac{1}{V_m} + \frac{1}{V_r}} \qquad (7)$$

Where: V_r and V_m represent the maximum kinetic corrosion rate of proton corrosion, and a mass transfer rate of the dissolved CO$_2$. The equation for the proton reaction controlled part is [26]:

$$\log(V_r) = 4.84 - \frac{1119}{T+273} + 0.58 \log(f_{CO_2}) - 0.34\,(PH_{actual} - pH_{CO_2}) \qquad (8)$$

Moreover, for the part controlled by mass transfer:

$$V_m = 2.8 \frac{U^{0.8}}{d^{0.2}}\, f_{CO_2} \qquad (9)$$

Where,
T : Temperature (^{o}C),
U : The velocity of crude oil (m/s).
d: Pipe diameter in (m).
pH_{CO_2}: The pH of pure water saturated with CO$_2$.
f_{CO_2}: The fugacity of the CO$_2$ (bar).
pH_{actual}: The pH resulting from the presence of dissolved salts.

The result from the Eq.(7) is adjusted by the use of a number of multiplying factors for the presence of a protective scale (F_{scal}), H$_2$S gas (F_{H_2S}) and crude oil (F_{oil}) on the base CO$_2$ corrosion rate as followers:

$$Corrosion\, rate = V_{cor.} * F_{scal} * F_{H_2S} * F_{oil} \qquad (10)$$

Where:

$$\log(f_{scal}) = \frac{2400}{T+273} - 0.61 \log(f_{co_2}) - 6.7 \qquad (11)$$

$$F_{H_2S} = \frac{1}{1 + 1800 \frac{P_{H_2S}}{P_{CO_2}}} \qquad (12)$$

$$F_{oil} = 0.059 \frac{W_{H_2O}}{W_{break}} U_{oil} + \frac{1.1 * 10^{-4}}{(W_{break})^2} \frac{\alpha}{90} + 0.059 \frac{W_{H_2O}}{W_{break}} U_{oil} \frac{\alpha}{90} \qquad (13)$$

And

$$W_{break} = -0.0166 * API + 0.83 \qquad (14)$$

Where,

$\propto$: The angle of deviation from vertical.

W_{H_2O}: Water friction in crude oil.

P_{CO_2}: Partial pressure of CO_2 gas in (bar).

P_{H_2S}: Partial pressure of H_2S gas in (bar).

API: The American Petroleum Institute gravity.

The partial pressure of dissolved CO_2 gas was calculated using Henry's law as followers [27]:

$$K_h = \frac{P_{CO_2}}{[CO_2]} \tag{15}$$

Where,

K_h : Henry's constant 29.76 atm/ mol.lit.

$[CO_2]$: The concentration of dissolved CO_2 gas in mol/lit.

3.2. Fugacity of CO_2 Dissolved Gas (f_{CO_2})

The fugacity of CO_2 (f_{CO_2}) is similar to its effective partial pressure and its expressed in Pa or atm., but corrected for non-ideality at high pressure and temperature. The basic equation for the correction of CO_2 fugacity used in ECE software given as followers [28]:

$$\log(f_{CO_2}) = \log(P_{CO_2}) + \left(0.0031 - \frac{1.4}{T+273}\right)P \tag{16}$$

In ECE V.5.1, the maximum total pressure P is limited to 250 bar and the equation is adjusted slightly for temperatures above 80°C by scale factors to provide a better fit in the fugacity curves.

4- Results and Discussion

The open circuit potentials or so called corrosion potential ($E_{cor.}$) of API 5L X60 and API 5L X80 carbon steel obtained from open circuit potential are illustrated in Table 6 at temperature 30°C. The Potentiostatic test begins at a temperature of 30°C due to the small values of corrosion potential obtained at 25°C and it is not appropriate to conduct the tests. As shown in Table **6**, the potential of the open circuit for different types of crude oil and steel has varied. Increasing the potential for corrosion shows an improvement in the performance of corrosion protection since the electrons transferred from the samples have decreased. The crude oil from Noor field has the lower potential, while crude oil from Halfaya field has the largest value; other crude oils types have moderate values.

Fig. **4** shows polarization curves obtained from Potentiosatic test under static and flow condition of crude oil at 1 m/s and temperature 30°C of the materials API 5L X60 and X80 carbon steel in the Noor crude oil. The slope of the polarization curves illustrated the velocity of reactions of the specimen's surface with crude oil impurities. Both pipeline materials showed large oscillations of applied potential with measured current, and as the applied potential increased, the curve fluctuations increased.

It also notes that a small change in the potential (ΔE) leads to a significant change in the current (ΔI), which means that the velocity of the corrosion reaction is high. The polarization curve obtained from testing of X60 steel in this type of crude oil showed a significantly large change in curves, which is attributed to the high reaction speed and then the transfer of electrons is larger than X80 steel. As indicates in the polarization curve the X60 steel shows high corrosion speed compared to the X80 steel.

Table 6. Open circuit potential (corrosion potential ($E_{cor.}$) in mV) obtained from Potentiostatic test at T = 30°C

Steel types	Crude oil types					
	Halfaya	Faqa 1	Abu Gharab	Faqa 2	Bazurkan	Noor
Static case						
API 5L X80	-87	-104	-119	-133	-151	-160
API 5L X60	--130	-151	-163	-176	-198	-210
Flow case (1m/s)						
API 5L X80	-116	-136	-148	-161	-169	-180
API 5L X60	-160	-181	-201	-214	-227	-240
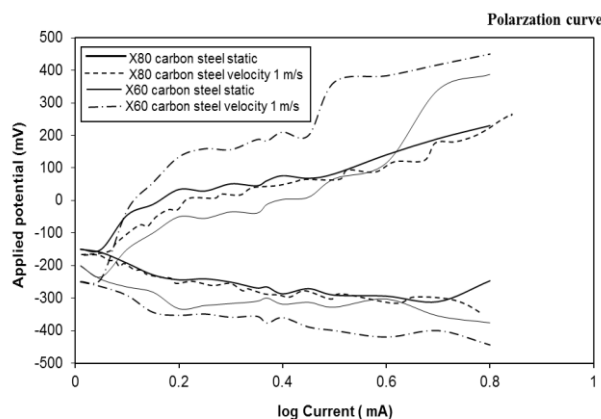
Fig. 4. Polarization curves under static and flow conditions in Noor crude oil at 30°C

By varying the temperature and types of crude oil and conduct the Potentiostatic corrosion analogue polarization curves of Fig.4 can be obtained. To obtain the corrosion current using the Tafel method, the polarization curves of Fig. **4** were analyzed. This was done using the software version 5.1.exe of the M-Lab science program to obtain the corrosion current. The equivalent weight of carbon steel X60 and X80 is calculated using Eq.(3) and the value of the corrosion rate is calculated using Eq.(1) at a constant temperature. The final results of the conclusions are illustrated in Fig. **5** A to F.

Fig. **5** A to F show the rate of corrosion vs. temperature obtained from Potentiostatic test the pipeline materials in the six types of crude oils. Comparing the rates of corrosion results between these fields, it was found that the crude oil from Noor field shows the highest rate of corrosion, while crude oil from Halfaya field shows the least values; other crude oils show moderate values.

The rates of corrosion differ may be because the crude oil from Noor field has the highest water and impurities as given in Table **4** and Table **5**. Both pipeline materials have a steady value of increases in the corrosion rate during the increases in temperature.

The results of testing in the flow crude oil indicate that the corrosion current is significantly increased due to the effect of the crude oil velocity factor, which contributes to increasing the diffusion of different ions in steel surfaces during the test.

Table **7** shows a comparison of the rate of corrosion between the two carbon steel materials API 5L X60 and API 5L X80 tested in the six types of crude oils at 30°C. As shown in Table 7, when both materials tested in crude oil from Noor field, the carbon steel API 5L X60 has a corrosion rate of 0.190 mm/y and 0.295 mm/y in static and flow cases respectively, while the carbon steel API 5L X80 has a corrosion rate of 0.156 mm/y and 0.263 mm/y in static and flow cases respectively. The results of the test in crude oil from Halfaya field show that the carbon steel API 5L X60 has a corrosion rate of 0.081 mm/y and 0.092 mm/y in static and flow cases respectively, while API 5L X80 carbon steel has a corrosion rate of 0.042 mm/y and 0.053 mm/y in static and flow cases respectively. Other types of crude oils have moderates corrosion rate values.

The crude oil flow is effects on the rate of corrosion by different methods. Compared to the static case, the corrosion ion and impurities transport in crude oil increases with crude oil flow. This accelerates the corrosion reaction within pipelines. Therefore, the rate of corrosion increased in case of flow compared to the static case. The flow effect on the inhibition element, in particular asphalt, which is collected at the bottom of the pipeline surface and thus weakens the inhibition element.

On the other hand, higher crude oil flow leads to higher turbulence, which increases the wall shear stress and further increases the pipeline corrosion rate. The scouring effect of high-speed oil flows can quickly destroy films of corrosion products or prevent the formation of films due to corrosion, which reduces the effect of corrosion inhibitors. In static cases, the rate of corrosion is lower because the oil film protects the surface of the specimen from corrosion by reduces the contact of impurities and ions with the specimen surfaces.

The conductivity of crude oils is one of the important factors affecting the corrosion rate values during the Potentiostatic test. It has depended on various factors including; water percent temperature, metal concentration, ion concentration, and presence of organic matter, dissolved gases and pH values. The current is relatively high at the start of the test and then started to decrease to lower steady values, this is due to ions and compounds that support corrosion reactions is removed and consumption.

As the temperature of crude oil increases, the ions contained in crude oil contribute to increase the flow of electrons and move more freely through crude oil to the reference electrode and increase the oxidation and reduction processes, leading to faster rates of corrosion.

Noor crude oil has the highest amount of metal compositions and water percent compared to other crude oils as given in Table **4**.

Chloride salts such as $NaCl$, $CaCl_2$, $MgCl_2$, it is found in crude oil with different concentrations. As the temperature or flow of crude oil increases, the mixture of this chloride salts with water in crude oil and hydrolysis increases. The hydrolysis of chloride salts in water leads to the initiation of a strong HCl acid, which increases the acidity of crude oil (pH value) and enhances the rate of corrosion. Chloride salt hydrolysis can be administered by the following reactions [25]:

$$NaCl + H_2O \longrightarrow NaOH + HCl \qquad (17)$$

$$MgCl_2 + 2H_2O \longrightarrow Mg(OH)_2 + 2HCl \qquad (18)$$

$$CaCl_2 + 2H_2O \longrightarrow Ca(OH)_2 + 2HCl \qquad (19)$$

The chloride salt NaCl and kinematics viscosity for Noor oilfields are 44 ppm and 35.5 cst, respectively, according to Table 4. Since the viscosity is low; this made the flow of crude oil is easily compared to other types. It also increases the contact of impurities contained in crude oil with the internal surface of pipelines leading to a faster rate of corrosion.

Table 7. Corrosion rate values in (mm/year) obtained from test at $T = 30°C$

Static case						
Steel type	Crude oil types					
	Halfaya	Faqa 1	Abu Gharab	Faqa 2	Bazurkan	Noor
API 5L X80	0.042	0.059	0.094	0.116	0.132	0.156
API 5L X60	0.053	0.069	0.121	0.134	0.15	0.190
Flow case (1m/s)						
API 5L X80	0.081	0.130	0.152	0.163	0.204	0.263
API 5L X60	0.092	0.110	0.164	0.186	0.243	0.295

To illustrate the effect of concentration of CO_2 and H_2S dissolved gases in corrosion rate, engineering corrosion software (ECE) was used to calculate the corrosion rate at various temperatures for both types of pipeline material. The rate of corrosion for each type of steel tested in each type of crude oils is estimated at a constant temperature for a pipeline length of 100 m.

For executing the ECE software program, the total pressure was taken as 50 bar and the pressure of dissolved CO_2 gas was calculated according to the concentration of CO_2 dissolved gas in each type of crude oils using Eq.(15). Then, the corrosion rate in the range of temperatures from 20°C to 65°C was obtained from ECE software program and drawn as a function of temperatures in Fig. **6**.
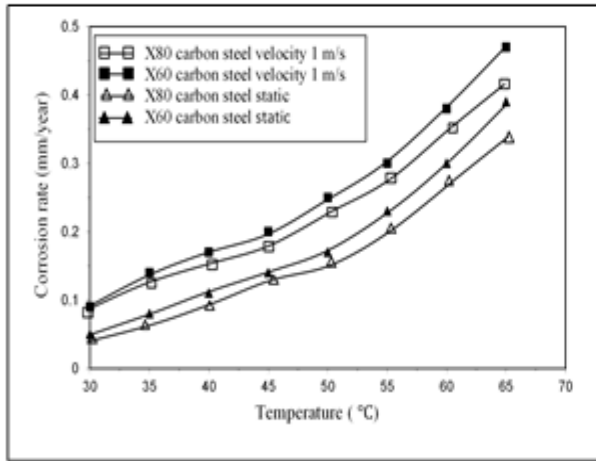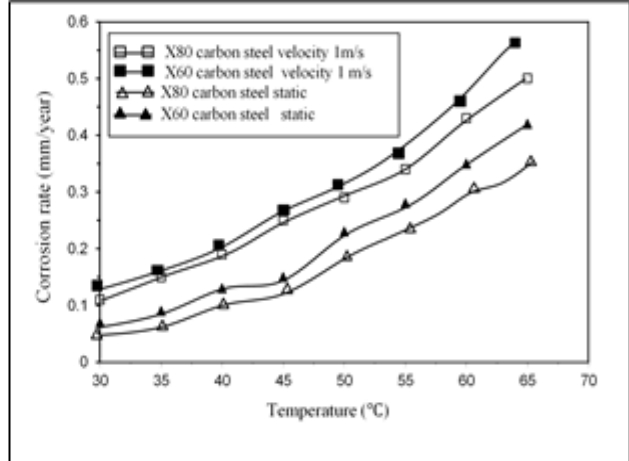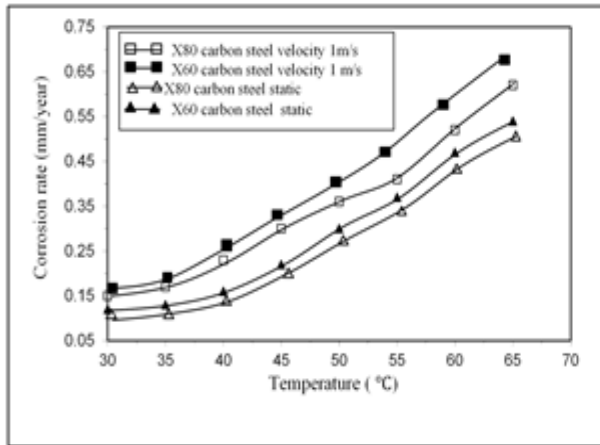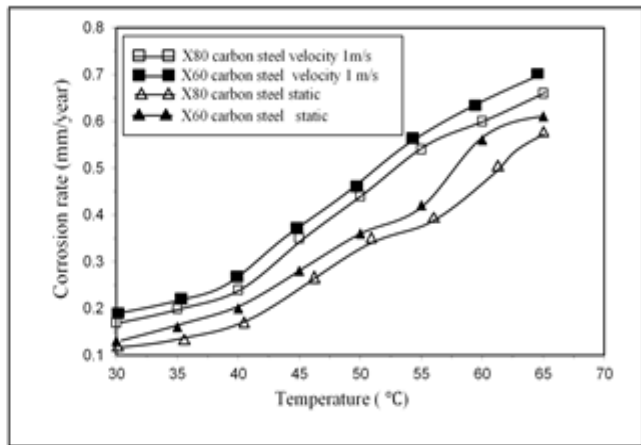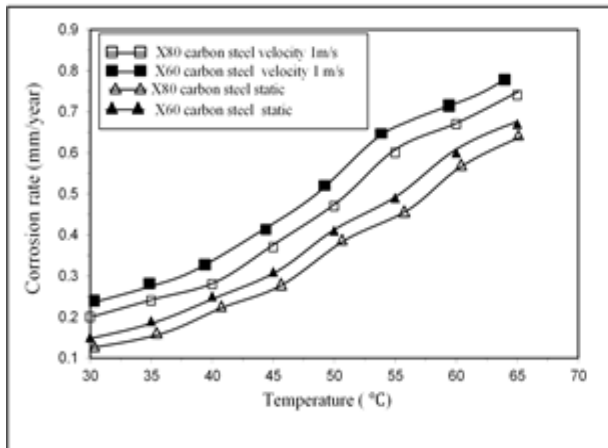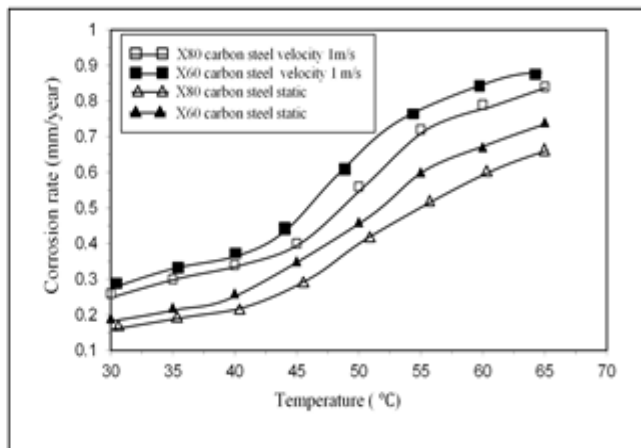
Fig. 5. Corrosion rate vs. temperature for fields: A- Halfaya   B-Faqa 1   C- Abu Gharab   D-Faqa 2 E- Bazurkan F- Noor

As indicated in Fig. **6**, due to the low concentration of dissolved gasses CO_2 and H_2S, which listed in Table 4, the corrosion rate is very small. Most corrosion rate occurs due to the effect of water and other impurities of crude oil in addition to the operating condition include temperature and pressure in pipes.

The CO_2 gas mixture with water forms weak carbonic acid (H_2CO_3) for both cases of static and flow, but the flow of crude oil has improved reactions, the transfer of ions and carried out more corrodes species to the exposure area of the steel specimen, this caused higher rates of corrosion. In general, both CO_2 and H_2S gasses in water were analyzed to form cations and anion compounds, and these increased reactions occurred in the anode and cathode parts of the Potentiostatic test. The following equations are illustrated the analyzed dissolved gasses CO_2 and H_2S in water:

$$CO_2 \text{ (g)} + H_2O \text{ (L)} \rightleftharpoons H^+ \text{ (aq)} + HCO_3 \text{ (aq)} \quad (20)$$

$$H_2S \text{ (g)} + H_2O \text{ (L)} \rightleftharpoons HS^- \text{ (aq)} + H_3O^+ \text{ (aq)} \quad (21)$$

Fig. 6. Effect of CO_2 on corrosion rate at various temperatures for fields: A- Bazurkan   B- Noor   C- Faqa 2   D- Abu gharab   E- Faqa 1   F- Halfaya
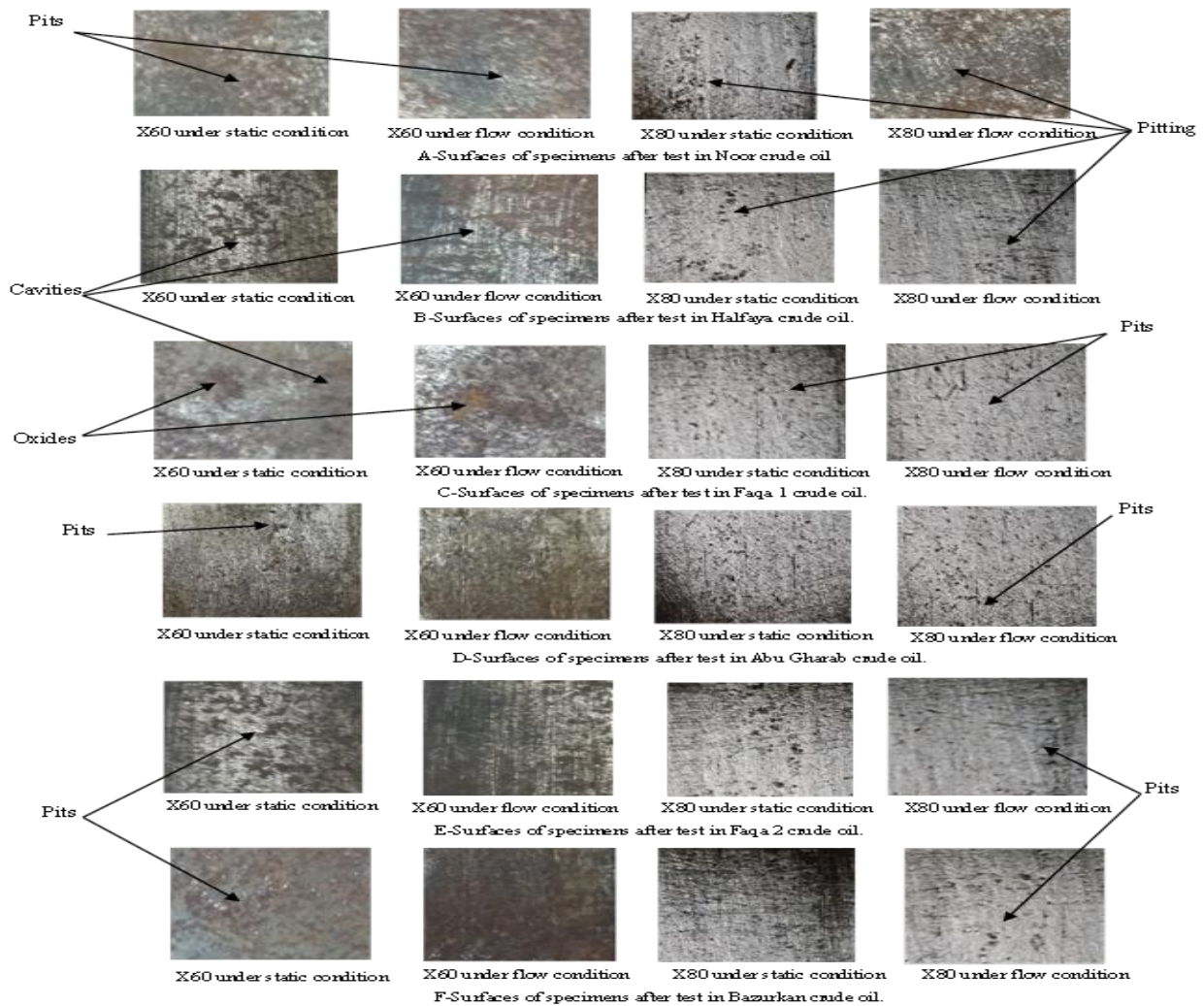
Fig. 7. Surfaces of specimens after test in the six different types of crude oils

Fig. **7** illustrates the microscopic surface of specimens after conducted the Potentiostatic test in the six types of crude oil at ambient temperature. To remove crude oil deposits on the specimen's surface, kerosene was used to clean the specimens. There are two types of localized corrosion, pitting and general corrosion. The images of the surface of the specimens in Fig. **7** after the Potentiostatic test in static and flow conditions show that a rough and porous surface was produced, i.e. numerous cavities with small pits covering the surfaces. In the case of a flow condition, the number of cavities and pits are visually higher than that in a static condition due to the effect of flow.

It is clear from the surface microstructures of Fig. **7**, X60 shows more surface damage under flow conditions than in static conditions, and the pits were uniformly distributed over the surface, which was surrounded by a small area of corrosion. It also indicates the formation of oxides layer spread on the steel surface at various points obtained following a Potentiostatic test in crude oil solutions. A comparison of the specimen's surfaces between static and flow conditions, it shows that the actual corrosion pits have more complex geometries in flow conditions with different pit depths and length than in static cases.

5- Conclusions

Based on the results of this study, the following concluded are obtained:

1- The result of the Potentiostatic polarization tests showed that the polarization curves have a significant large oscillation associated with the initiation of unstable pits and high electrical resistance of crude oils.
2- The corrosion rate of CO_2 and H_2S dissolved gases obtained from ECE software program is minimal due to the small concentration of CO_2 and H_2S dissolved gases in the tested crude oil.
3- The X80 carbon steel has lower corrosion values, while the X60 carbon steel has largest values.
4- Noor crude oil has the highest corrosion rate value, while Halfaya crude oil has the lowest value; another crude oil has moderate values.
5- The corrosion rate in case of crude oil flow is larger than that obtained at static.
6- The surface of the samples tested showed pits and cavities covered the surfaces and both materials showed more damage in the surfaces under flow conditions than in a static case.

Acknowledgments

References

[1] J. Enani, "Corrosion control in oil and gas pipelines", International Journal of Scientific & Engineering Research, 2016, Vol.7, Issue 4, pp.1161-1164.

[2] S. Nesic, "Key issues related to modeling of internal corrosion of oil and gas pipelines - a review", Corrosion Science, 2007, Vol.49, pp.4308–4338.

[3] A. S. Yaro and K. H. Rashid , "Modeling and optimization of carbon steel corrosion in CO_2 containing oilfield produced water in presence of HAc", Iraqi Journal of Chemical and Petroleum Engineering, 2015, Vol.16, No.2, pp.1- 8.

[4] L. M. Smith and de Waard K., "Corrosion prediction and materials selection for oil and gas producing environments", Corrosion 2005, paper 05648: NACE International.

[5] L. Esteves, M. Cardosoa and V. Linsa, "Corrosion behavior of duplex and lean duplex stainless steels in pulp mill", Materials Research, 2018, Vol.21, No.1, pp.1-9.

[6] Q. Sulaiman , A. Al–Taie, D. M. Hassan, "Evaluation of sodium chloride and acidity effect on corrosion of buried carbon steel pipeline in iraqi soil", 2014, Iraqi Journal of Chemical and Petroleum Engineering, Vol.15 No.1, pp.1-8.

[7] A. K. Vuppu and W. P. Jepson, "The effect of temperature in sweet corrosion of horizontal multiphase carbon steel pipelines", Paper No. SPE-28809-MS, SPE Asia Pacific Oil and Gas Conference, 7-10 November, Melbourne, Australia, 1994.

[8] L. Xu and X. Wang, "The research of oil and gas pipeline corrosion and protection technology", Advances in Petroleum Exploration and Development, 2014, Vol.7, pp.102-105.

[9] Prakash, S. Surya, et al. "Internal Corrosion Management of Crude Pipelines." *2014 10th International Pipeline Conference*. American Society of Mechanical Engineers, 2014.

[10] T. A. Saleh, S. Husain Sahi and L. S. Mohamed. "Corrosion of electrical submersible pumps (ESP) in south Rumaila oil field", Iraqi Journal of Chemical and Petroleum Engineering, 2015, Vol.16, No.1, pp.63- 69.

[11] Z. M. Wang and J. Zhang, "Corrosion of multiphase flow pipelines: the impact of crude oil", Corros. Rev., 2016, Vol.34, No.2, pp.17-40.

[12] H. J. Muhammed, "Effects of soil properties on corrosion of soil pipeline at north of Iraq", M.Sc. Thesis, Mechanical Engineering Department, Near East University, Erbil, 2016.

[13] H. S. Mobbassar and A. M. Abdullah, "Corrosion of general oil-field grade steel in CO_2 environment update the light of current understanding", Int. J. Electchem. Sci., 2017, Vol.12,

[14] N. I. Mursalov, "Characteristic and mechanism of hydrogen sulfide corrosion of steel", The Journal of Processes of Petrochemistry and oil Refining (PPOR), 2017, Vol.18, pp.215-228.

[15] M. L. Cedeño, E. L. Vera and Y. T. Pineda, "Effect of contents oil temperature and flow rate in the electrochemical corrosion of the AISISAE1020-steel", IOP Conf. Series786, Journal of Physics, 2017, pp.1-8.

[16] F. Kolawole, S. Kolawole, J. Agunsoye, J. Adebisi, S. Bello and S. Hassan, "Mitigation of corrosion problems in API 5L steel pipeline-a review", J. Mater. Environ. Sci., 2018, Vol.9, N0. 8, pp. 2397-2410.

[17] API 5L X80 carbon steel specification data sheet, Report of the Henan BEBON International Co. Ltd., 2015, Chaini.

[18] API 5L X60 carbon steel specification data sheet, Report of the Henan BEBON International Co. Ltd., 2016, Chaini.

[19] ASTM G1-03, Standard Practice for Preparing, Cleaning, and Evaluating Corrosion Test Specimens, Report of ASTM 2011.

[20] ASTM G59-97, Standard Test Method for Conducting Potentiodynamic Polarization Resistance Measurements, Report of ASTM, USA, 2014.

[21] A. C. Potter, "Crude oil conductivity presentation", Report of Nalco Energy Service, 2007.

[22] G-102, Standard practice for calculation of corrosion rates and related information from electrochemical measurements, Report of ASTM, USA, 1999.

[23] O. N. Sylvester, O. N. Celestine, O. G. Reuben and C. E. Okechukwu, "Review of corrosion kinetics and thermodynamics of CO_2 and H_2S corrosion effects and associated prediction/evaluation on oil and gas pipeline system", Int. J. of Sci. & Tech. Res., 2012,Vol.1, pp.1-17.

[24] C. de Waard, and L. M. Smith and B. D. Criag, "The influence of crude oil on well tubing corrosion rate", NACE Corrosion Conference, paper No.03629, 2003.

[25] C. de Waard, U. Lotz and A. Dugstad, "Influence of liquid velocity on CO_2 corrosion: a semi-empirical model", NACE Corrosion 95, paper No. 128.

[26] M. H. Abbas, "Modeling CO_2 corrosion of pipeline steels", Ph.D., School of Marine Science and Technology, Newcastle University, USA. 2016.

[27] P. S. Brown, "Optimizing the long-term capacity expansion and protection of Iraqi oil infrastructure", M.Sc. Thesis, Naval Postgraduate School, Monterey, California, USA, 2005.

[28] M. R. Gray, P. E. Eaton and T. Le, "Kinetics of hydrolysis of chloride salts in model Crude Oil", Petroleum Science and Technology, 2008, Vol.26, No.16, pp.1924-1933.

تقييم تاثير السرعة والحرارة على معدل التاكل في انابيب النفط الخام بوجود الغازات المذابة CO2/H2S

الخلاصة

في هذا البحث، تم دراسة تأثير الغازات المذابة CO_2/H_2S وسرعة النفط الخام على معدل التأكل في الانابيب المستخدمة في نقل النفط الخام من ستة حقول مختلفة في محافظة ميسان جنوب العراق وهي (نور، بزركان، الحلفاية، ابو غريب، وحقول فكه1 وفكه2). اجريت الاختبارات العملية باستخدام طريقة الجهد الساكن على نوعين من انابيب الصلب الكربوني وهما API 5L X60 و API 5L X60. استخدم البرنامج الكتروني ECE لحساب معدل التأكل وتقيم تأثير كل من الضغط الجزئي لغاز CO_2، تركيب النفط الخام، سرعة النفط الخام ونسب العناصر المكونة للصلب على معدل التأكل. بينت النتائج العملية ان الصلب الكربوني من نوع API 5L X80 اظهر مقاومة اعلى للتأكل مقارنة بالصلب الكربوني API 5L X60. كما ان معدل التأكل في حالة الجريان يكون اكبر منه في حالة السكون. اظهر النفط الخام من حقل نور اعلى قيمة لمعدل التأكل، بينما النفط الخام من حقل الحلفاية امتلك اقل قيمة، النفط الخام من الحقول الاخرى امتلك قيم متوسطة من معدلات التأكل.